Magnetic impurities in half-integer-spin Heisenberg antiferromagnetic chains

Sebastian Eggert
Department of Physics, University of British Columbia, Vancouver, British Columbia, Canada V6T 1Z1

Ian Affleck
Department of Physics and Canadian Institute for Advanced Research, University of British Columbia, Vancouver, British Columbia, Canada V6T 1Z1

(Received 29 May 1992)

We study the effect of an isolated impurity on the low-energy properties of a half-odd-integer-spin Heisenberg antiferromagnetic chain using both numerical and conformal field theory techniques. The impurity corresponds to the substitution of a magnetic ion by a different ion with the same or different spin, or else to the coupling of a magnetic impurity to a single spin on the chain. Depending on which kind of impurity is present, the low-energy behavior corresponds either to a "healing" of the defect or else to a severing of the chain at the impurity location. In both cases there is a coupling-dependent length scale over which magnetic screening takes place. Analogies with the Kondo effect are elucidated.

I. INTRODUCTION

In this paper, we consider a large variety of types of magnetic and nonmagnetic defects in a Heisenberg antiferromagnetic chain. The simplest case corresponds to changing the strength of a single link (see Fig. 1). A more interesting case corresponds to changing the strengths of two adjacent links, which remain equal to each other (see Fig. 2). This could result from substituting another $s = \frac{1}{2}$ ion for a chain ion. The latter case can be generalized to the substitution of an impurity with $s > \frac{1}{2}$ (Fig. 3). Finally, we consider the coupling of a magnetic impurity of arbitrary s to a single chain-spin (Fig. 4). There are several motivations for this work.

Recently, an approach to the Kondo effect has been developed,[1,2] based on the separation of charge and spin degrees of freedom in the one-dimensional (1D) electron gas. (The Kondo effect is fundamentally one dimensional, since it involves only the s-wave channel.) The one-impurity Kondo effect only involves the spin degrees of freedom of the electron gas; at low energies the charge degrees of freedom are unaffected by the interaction. The spin degrees of freedom of the one-dimensional electron gas at low energies are identical to those of the half-integer-spin Heisenberg antiferromagnet. Hence it is natural to look for a "stripped down" version of the Kondo effect involving a magnetic impurity interacting with the Heisenberg chain.

The effect of an isolated impurity has been studied recently[3] in *integer-spin* antiferromagnetic chains, which exhibit the Haldane gap, in the *bulk* excitation spectrum. It was shown that an open $s = 1$ chain has effective $s = \frac{1}{2}$ degrees of freedom at each end, whose mutual coupling vanishes exponentially with chain length. These excitations are localized within a distance of the order of the correlation length ξ (about 7) from the ends of the chain. A magnetic impurity *weakly coupled* to a long chain of length $L >> \xi$ can be described simply in terms of its coupling to the effective $s = \frac{1}{2}$ degree of freedom at the chain end. The half-integer case is much different since there is no gap for bulk excitations and the correlation length is infinite. The effect of a magnetic or nonmagnetic impurity now propagates into the chain a distance which is determined by the strength of the coupling and diverges as the coupling goes to zero as in the Kondo effect.

Some of these problems have been considered previously and independently in a recent discussion of tunneling in one-dimensional quantum wires.[4,5] One-dimensional spinless fermions are equivalent to the xxz $s = \frac{1}{2}$ quantum spin chain. The Heisenberg model corresponds to a particular (repulsive) value of the interaction strength. A single altered link corresponds to the generic tunneling problem. Two adjacent modified links

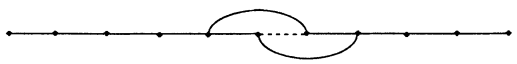

FIG. 1. A quantum spin chain with one altered nearest-neighbor link. We also modify the next-nearest-neighbor couplings shown to preserve the ratio $J_2/J = 0.24$. See discussion in Sec. III.

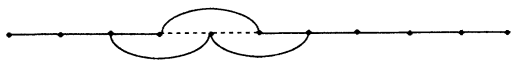

FIG. 2. A quantum spin chain with two altered nearest-neighbor links. We also modify the next-nearest-neighbor couplings shown to preserve the ratio $J_2/J = 0.24$. See discussion in Sec. III.

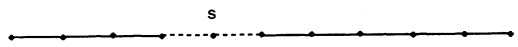

FIG. 3. A quantum spin chain with an internal impurity of size s. In this case the impurity has no next-nearest-neighbor couplings.

correspond to resonant tunneling. Our results provide numerical evidence for conjectures made in those papers.

Just as in the Kondo effect, the renormalization group provides the appropriate language for describing these systems. The scale and conformal invariance of the pure chain at low energy is broken by the coupling to the impurity. This effective coupling may grow or shrink as we lower the energy scale; eventually, at zero energy, the system renormalizes to a stable fixed point. Recent progress by Cardy[6] in the renormalization-group theory of two-dimensional critical systems with boundaries has been used to study quantum impurities.[1,2] Quantum impurities in spin chains provide a relatively simple illustration of these techniques. In the simplest version of the Kondo effect, the stable fixed point is of the local Fermi-liquid variety; i.e., it is equivalent to a simple boundary condition on otherwise free fermions, corresponding to a $\pi/2$ phase shift, with the screened impurity removed from the low-energy effective Hamiltonian. In the spin-chain problems considered here the stable fixed points also correspond to simple boundary conditions on otherwise unperturbed chains. The two types of boundary conditions that occur correspond to having no impurity, i.e., no boundary, or else to cutting the chain at the impurity site as would occur with the insertion of a nonmagnetic impurity into the chain. Low-temperature local properties, such as the impurity susceptibility, are governed by the leading irrelevant operator at the stable fixed point, as in the Kondo effect. The dimensions of these operators are, in general, different than in the simplest version of the Kondo effect, so the analogy does not hold in complete detail.

We analyze these problems using two powerful techniques: the renormalization group, and numerical finite-size scaling. The first approach allows a complete description of the vicinity of either fixed point (no boundary or severed chain). A complete description of all operators and their scaling dimensions is known at these fixed points. This allows us to determine which types of impurity interactions are relevant or irrelevant. It also permits us to make educated guesses about the flow between these two fixed points, although the crossover regime is beyond the control of these methods. The second technique is based on calculating the energies of a few low-lying states

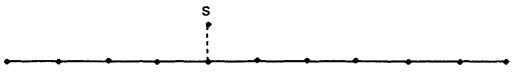

FIG. 4. A quantum spin chain with an external impurity of size s.

of the system for a range of lengths, $l \leq 23$. The low-energy spectrum of the continuum model consists of infinite towers of states with spacings of order $1/l$. This infinite set of energies is known (up to an overall scale factor, the spin-wave velocity) at the two fixed points. Thus we can test whether the spectrum approaches that of the conjectured stable fixed point, up to corrections which vanish faster than $1/l$. These corrections are predicted to vanish as $1/l^{1+d}$ where d is the dimension of the leading irrelevant coupling constant,[7] a conjecture which can also be checked numerically.

The rest of the paper is organized as follows. In the next section we review the bosonization approach to the continuum limit of quantum spin-$\frac{1}{2}$ chains. This discussion includes the presence of a marginal operator and a procedure to circumvent the resulting problem of logarithmically slow scaling in finite-size numerical work. We also derive the asymptotic finite-size spectrum for even or odd length chains with periodic or free boundary conditions as well as the dimensions of the various relevant and irrelevant operators, which are important in our study of impurities. In Sec. III we make predictions concerning the effect on the finite-size spectrum of the various types of impurities mentioned above and make detailed comparisons with the numerical results. In Sec. IV we discuss the thermodynamics of these systems. They provide instructive examples of systems with noninteger "ground-state degeneracy."[2] The impurity specific heat and susceptibility are determined by the leading irrelevant operators as in the Kondo effect.[14] In Sec. V we summarize our results and contrast these systems to the Kondo problem. Some comments are made concerning the effect of a finite density of impurities.

II. BOSONIZATION AND QUANTUM FIELD THEORY PREDICTIONS

In this section we review how quantum field theory methods are used to describe the low-temperature physics of the Heisenberg spin-$\frac{1}{2}$ chain with periodic or free boundary conditions. The Hamiltonian is

$$H = \sum_{i=1}^{l-1} \left(\frac{J}{2} (S_i^+ S_{i+1}^- + S_i^- S_{i+1}^+) + J_z S_i^z S_{i+1}^z \right) \qquad (2.1)$$

for the case of free boundary conditions. (We take $J > 0$.) For periodic boundary conditions the lth and first site are also coupled with the same coupling constants, J and J_z.

A. Bosonization

We can now apply the Jordan-Wigner transformation by expressing the spin operators in terms of fermion annihilation and creation operators at each site, resulting in a spinless fermion Hamiltonian:[8]

$$S_i^z = \psi_i^\dagger \psi_i - \tfrac{1}{2}, \qquad (2.2)$$

$$S_i^- = (-1)^i \psi_i \exp\left(i\pi \sum_{j=1}^{i-1} \psi_j^\dagger \psi_j \right), \tag{2.3}$$

$$H = \sum_{i=1}^{l-1} \Big(\frac{J}{2} (\psi_i^\dagger \psi_{i+1} + \text{H.c.}) + J_z (\psi_i^\dagger \psi_i - \tfrac{1}{2})(\psi_{i+1}^\dagger \psi_{i+1} - \tfrac{1}{2}) \Big). \tag{2.4}$$

We then restrict the Hamiltonian to low-energy excitations and go to the continuum limit to obtain an effective low-energy theory, described by a (1+1)-dimensional field theory Hamiltonian of left- and right-moving fermions.[8] The $S^z S^z$ interaction can be expressed in terms of the fermion currents $J_I = :\psi_I^\dagger \psi_I:$, $I = L, R$ and contributes partly to the free part of the resulting Hamiltonian, because we can rewrite the derivative terms to first order as

$$\psi_R^\dagger i \frac{d}{dx} \psi_R \approx \pi J_R J_R, \tag{2.5}$$

$$\psi_L^\dagger i \frac{d}{dx} \psi_L \approx -\pi J_L J_L, \tag{2.6}$$

up to an (infinite) constant. The resulting Hamiltonian is

$$H = v \int dx \left[\psi_R^\dagger i \frac{d}{dx} \psi_R - \psi_L^\dagger i \frac{d}{dx} \psi_L + 2\pi b J_L J_R \right] \tag{2.7}$$

$$= \pi v \int dx \left[J_R J_R + J_L J_L + 2b J_L J_R \right], \tag{2.8}$$

where b is a constant of order J_z and v is the renormalized "speed of light." Here all operators which are irrelevant at low energies in the limit where J_z is small have been dropped. This model can be transformed using the Abelian bosonization rules:[8]

$$J_L = \frac{1}{\sqrt{4\pi}} \left(\Pi_\phi - \frac{\partial \phi}{\partial x} \right), \quad J_R = -\frac{1}{\sqrt{4\pi}} \left(\Pi_\phi + \frac{\partial \phi}{\partial x} \right), \tag{2.9}$$

$$\psi_R \propto \exp(i\sqrt{4\pi}\phi_R), \quad \psi_L \propto \exp(-i\sqrt{4\pi}\phi_L).$$

The resulting Hamiltonian is a noninteracting boson theory

$$\mathcal{H} = \frac{v}{2} \left[(1-b)\Pi_\phi^2 + (1+b) \left(\frac{\partial \phi}{\partial x} \right)^2 \right]. \tag{2.10}$$

Here Π_ϕ is the momentum variable conjugate to ϕ; ϕ_L and ϕ_R are the left- and right-moving parts of ϕ:

$$\phi = \phi_L + \phi_R. \tag{2.11}$$

The boson operators now have to be transformed by a canonical transformation to obtain a conventionally normalized theory:

$$\phi \to \frac{\phi}{\sqrt{4\pi} R}, \tag{2.12}$$

$$\Pi_\phi \to \sqrt{4\pi} R \, \Pi_\phi,$$

$$v \to \sqrt{1-b^2}\, v, \tag{2.13}$$

$$R^2 = \frac{1}{4\pi} \sqrt{\frac{1+b}{1-b}} \approx \frac{1+b}{4\pi}, \tag{2.14}$$

$$\mathcal{H} = \frac{v}{2} \left[(\Pi_\phi)^2 + \left(\frac{\partial \phi}{\partial x} \right)^2 \right]. \tag{2.15}$$

With the help of the Bethe ansatz, the "boson radius" R as a function of J_z can be exactly determined to be[8]

$$R = \left[\frac{1}{2\pi} - \frac{1}{2\pi^2} \cos^{-1} \frac{J_z}{J} \right]^{1/2}, \tag{2.16}$$

which agrees to first order in J_z with the field theory calculations ($b = 2J_z/\pi J$).

B. Operators

By combining the spin to fermion and fermion to boson transformations we obtain the continuum limit representation for the spin operators:

$$S_j^z \approx \frac{1}{2\pi R} \frac{\partial \phi}{\partial x} + (-1)^j \text{const} \cos \frac{\phi}{R}, \tag{2.17}$$

$$S_j^- \approx e^{i2\pi R\tilde{\phi}} \left(\text{const} \cos \frac{\phi}{R} + (-1)^j \text{const} \right),$$

where R is given in Eq. (2.16). The boson ϕ must be thought of as a periodic variable measuring the arc length on a circle of radius R; i.e.,

$$\phi \equiv \phi + 2\pi R, \tag{2.18}$$

$$\tilde{\phi} \equiv \tilde{\phi} + 1/R, \tag{2.19}$$

where $\tilde{\phi}$ is the dual field defined in terms of the left- and right-moving components of ϕ by

$$\tilde{\phi} \equiv \phi_L - \phi_R. \tag{2.20}$$

The periodicity condition on $\tilde{\phi}$ follows from that on ϕ, as will be shown in Sec. II B. Note that these translations leave the spin-operators invariant. Correlation functions and the low-energy spectrum predicted by this theory indeed agree with the calculation from independent methods.[8]

There are two important independent discrete symmetries of the spin chain which we need to identify in the continuum limit. The first one is translation by one site, Tr. This appears as a discrete symmetry independent of translation in the continuum limit. We see from Eq. (2.17) that it corresponds to

$$\text{Tr} : \phi \to \phi + \pi R, \quad \text{Tr} : \tilde{\phi} \to \tilde{\phi} + 1/2R. \tag{2.21}$$

The second one is site parity, P_S, i.e., reflection about a site. Note that this *does not* interchange even and

odd sublattices. Thus it must map the spin operators into themselves. Since parity interchanges left and right, ϕ and $\tilde{\phi}$ transform oppositely. We see that the correct transformation is

$$P_S : \phi \to -\phi, \quad P_S : \tilde{\phi} \to \tilde{\phi}. \tag{2.22}$$

There is a third discrete symmetry, link parity, P_L, i.e., reflection about a link. However, this is not independent, but is a product of the other two. It corresponds to

$$P_L : \phi \to -\phi + \pi R, \quad P_L : \tilde{\phi} \to \tilde{\phi} + 1/2R. \tag{2.23}$$

In our discussion of impurities we will be interested in the continuum limit representation for $S_j^- S_{j+1}^+ + S_j^+ S_{j+1}^-$ and $S_j^z S_{j+1}^z$. The first operator is given by

$$S_j^- S_{j+1}^+ + S_j^+ S_{j+1}^- \approx i(-1)^j (\psi_L^\dagger \psi_R - \text{H.c.}), \tag{2.24}$$

ignoring derivative terms of higher dimension. Using the bosonization formula of Eq. (2.9) and rescaling the boson field following Eq. (2.12), we obtain

$$S_j^- S_{j+1}^+ + S_j^+ S_{j+1}^- \approx (-1)^j \text{const} \sin \frac{\phi}{R}. \tag{2.25}$$

The most relevant part of $S_i^z S_{i+1}^z$ is also the staggered part, i.e., the cross term between the uniform and staggered parts of S^z. A typical term is

$$: \psi_L^\dagger \psi_L : (x)\, \psi_L^\dagger \psi_R(x+a), \tag{2.26}$$

where we have introduced the lattice spacing a for the first time. This can be written as a completely normal ordered four-Fermion operator (which reduces to an irrelevant derivative operator as $a \to 0$) together with an additional term from Wick ordering of the form

$$\frac{-i}{2\pi a} \psi_L^\dagger \psi_R. \tag{2.27}$$

Combining all such terms together we obtain the same operator as in Eqs. (2.24) and (2.25), for all values of R. (While this follows from symmetry at the Heisenberg point, it is not *a priori* obvious in the general case.) These results can also be obtained by using the bosonic representation of the spin operators of Eq. (2.17) and the operator product expansion. The operator $\sin \phi/R$ has dimension $d = 1/4\pi R^2$; at the Heisenberg point, $d \to \frac{1}{2}$. (This is the so-called spin-Peierls operator which can be induced in the Hamiltonian by a staggered interaction.)

In Sec. III we will be concerned with spin chains obeying either periodic or free boundary conditions. We need to uncover the corresponding boundary conditions on the bosons in the continuum limit. In the periodic case, for even length l, it is clear from Eq. (2.17) that the boundary conditions on the boson are also simply periodic, i.e.,

$$\begin{aligned} &\phi(l,t) = \phi(0,t) + 2\pi R \mathcal{S}^z, \quad \mathcal{S}^z = 0, \pm 1, \pm 2, \dots, \\ &\tilde{\phi}(l,t) = \tilde{\phi}(0,t) + m/R, \quad m = 0, \pm 1, \pm 2, \dots . \end{aligned} \tag{2.28}$$

On the other hand, if the length l is odd, we see from Eq. (2.17) that the correct boundary conditions on the boson are *antiperiodic*; i.e., $\mathcal{S}^z$ and m are half integers. We see from Eq. (2.17) that $\mathcal{S}^z$ is the z component of the total spin:

$$\mathcal{S}^z \equiv \sum_i S_i^z. \tag{2.29}$$

It is integer or half integer for an even or odd length chain, respectively, as expected.

The case of free ends is slightly more subtle. One way of dealing with it is to introduce fermion fields on two additional "phantom sites" 0 and $l+1$, let the sum in Eq. (2.1) run from 0 to l, and then impose vanishing boundary conditions on ψ_0 and ψ_{l+1}. This imposes conditions on the continuum limit of left- and right-moving Fermion fields:

$$\begin{aligned} &\psi_L(0) + \psi_R(0) = 0, \\ &\psi_L(l+1) + (-1)^{l+1} \psi_R(l+1) = 0. \end{aligned} \tag{2.30}$$

Using the bosonization formulas of Eq. (2.9) and taking into account the fact that ϕ_L and ϕ_R do not commute, we conclude that the correct boundary conditions on the bosons are

$$\phi(0) = \pi R, \quad \phi(l) = 2\pi R(\mathcal{S}^z + \tfrac{1}{2}), \tag{2.31}$$

where $\mathcal{S}^z$ is integer or half-odd integer for l even or odd, respectively.

In Sec. III we will need the continuum representation of the spin operators near a free end. It is important to realize that the operators have a different scaling dimension near such a free end than they do in the bulk. This is an example of "boundary critical phenomena." In this case we may easily deduce the dimensions from the bosonic representation of Eq. (2.17) after imposing the boundary conditions $\phi(0,t) = \pi R$. Note that this implies $\phi_L(0,t) = \pi R - \phi_R(0,t)$ and hence $\tilde{\phi}(0,t) = 2\phi_L(0,t) - \pi R$. Since ϕ_L is a function only of $x - t$ and ϕ_R only of $x + t$, we conclude that

$$\phi_R(x,t) = -\phi_L(-x,t) + \pi R, \tag{2.32}$$

i.e., we may reflect the right-moving field to the negative x axis where we can regard it as minus the analytic continuation of the left moving field, shifted by πR. All operators can therefore be expressed in terms of left movers only.

The boundary operators can be written as

$$\begin{aligned} &S^z_{\text{bound}} \propto \frac{\partial \phi_L}{\partial x}, \\ &S^-_{\text{bound}} \propto e^{4\pi i R \phi_L}. \end{aligned} \tag{2.33}$$

These have scaling dimensions $d = 1$ and $d = 2\pi R^2$, respectively. To understand the meaning of these boundary

scaling dimensions, it is instructive to consider the staggered part of the spin-spin correlation function at the Heisenberg point. This is most easily calculated for S^- by using

$$S_j^- \propto (-1)^j e^{i2\pi R[\phi_L(x,t)-\phi_L(-x,t)]}. \tag{2.34}$$

The two-point function for S^- reduces to a four-point function for the left-moving factor, giving

$$\langle \mathbf{S}(t_1,x_1)\cdot\mathbf{S}(t_2,x_2)\rangle \propto (-1)^{x_1-x_2}\sqrt{\frac{x_1x_2}{[(x_1-x_2)^2-t_{12}^2][(x_1+x_2)^2-t_{12}^2]}}, \tag{2.35}$$

where we have set the spin-wave velocity to one and $t_{12}\equiv t_1-t_2$. Note that far from the boundary, when $x_1x_2 \gg |(x_1-x_2)^2-t_{12}^2|$, we recover the bulk correlation function $\propto 1/\sqrt{(x_1-x_2)^2-t_{12}^2}$, corresponding to a scaling dimension of $\frac{1}{2}$ for the staggered spin operator. However, the correlation function near the boundary (i.e. when $|t_{12}| \gg x_1, x_2$) takes the form $\propto \sqrt{x_1x_2}/|t_{12}|^2$, corresponding to a scaling dimension of 1 for the staggered boundary spin operator.

We will also need the continuum limit form of the spin dot product $\mathbf{S}_i\cdot\mathbf{S}_{i+1}$ at the boundary. It follows from Eq. (2.33) that this is simply $(\partial\phi_L/\partial x)^2$. This is the left-moving part of the Hamiltonian density T_L.

C. Non-Abelian bosonization and the marginal operator

The leading irrelevant operator, coming from Umklapp processes in the fermion representation, is $\cos(2\phi/R)$ of dimension $1/\pi R^2$. This becomes marginal at the isotropic (Heisenberg) point $R=1/\sqrt{2\pi}$, leading to a transition to the Néel ordered phase. A manifestly SU(2) symmetric continuum limit representation for the Heisenberg model is provided by non-Abelian bosonization. We now introduce an SU(2)-matrix bosonic field, g_β^α. Its action includes the Wess-Zumino term with coefficient $k=1$. g is related to the Abelian boson field ϕ by

$$g \propto \begin{pmatrix} ie^{i\sqrt{2\pi}\phi} & e^{i\sqrt{2\pi}\tilde{\phi}} \\ -e^{-i\sqrt{2\pi}\tilde{\phi}} & -ie^{-i\sqrt{2\pi}\phi} \end{pmatrix}. \tag{2.36}$$

The spin operators are now represented as

$$\mathbf{S}_j \approx (\mathbf{J}_L+\mathbf{J}_R) + \text{const}\, i(-1)^j \mathrm{tr}[g\boldsymbol{\sigma}], \tag{2.37}$$

where $\mathbf{J}_{L,R}$ are the left and right SU(2) currents (or spin densities)

$$\mathbf{J}_L \equiv \frac{-i}{4\sqrt{\pi}}\mathrm{tr}[g^\dagger\partial_- g\boldsymbol{\sigma}],\quad \mathbf{J}_R \equiv \frac{i}{4\sqrt{\pi}}\mathrm{tr}[\partial_+ g g^\dagger\boldsymbol{\sigma}]. \tag{2.38}$$

Translation by one site and site parity act on g simply as

$$\mathrm{Tr}: g\to -g,\quad P_S: g\to -g^\dagger. \tag{2.39}$$

The boundary spin operators of Eq. (2.33) have a simple expression in terms of left movers in the non-Abelian language:

$$\mathbf{S}_{\text{bound}} \propto \mathbf{J}_L. \tag{2.40}$$

The continuum limit boundary operator corresponding to $\mathbf{S}_i\cdot\mathbf{S}_{i+1}$ is $\mathbf{J}_L\cdot\mathbf{J}_L \propto T_L$.

The marginal interaction mentioned above is $\lambda\mathbf{J}_L\cdot\mathbf{J}_R$. [Actually $(J_L^+J_R^- + \text{H.c.})$ corresponds to $\cos\sqrt{8\pi}\phi$. The $J_L^zJ_R^z$ part of the interaction corresponds to $(\partial\phi/\partial t)^2 - (\partial\phi/\partial x)^2$.] This is marginally irrelevant for the Heisenberg model, corresponding to $\lambda<0$. Since the effective coupling constant $\lambda_{\text{eff}}(l)$ scales to zero logarithmically slowly with the length scale l, logarithmic corrections arise.[9] In particular, it makes an accurate determination of the critical behavior from finite-size scaling essentially hopeless unless exponentially large chains can be studied. Therefore, it is useful to add a next-nearest-neighbor interaction to the Heisenberg model:

$$H \to \sum_i (J\mathbf{S}_i\cdot\mathbf{S}_{i+1} + J_2\mathbf{S}_i\cdot\mathbf{S}_{i+2}). \tag{2.41}$$

The marginal coupling constant λ decreases with increasing J_2/J. It passes through 0 at a critical point which has been estimated numerically to be approximately 0.24.[10] For larger J_2/J the system is in a spontaneously dimerized phase. (In particular, at $J_2/J=\frac{1}{2}$ the exact ground states are the nearest-neighbor dimer states.) Right at the critical point the marginal operator is absent, and hence finite-size scaling becomes very accurate even with chains of modest lengths of order 20, since corrections drop off at least as fast as $1/l$. Therefore, most of the numerical work reported here has been done at this critical point. Note that the model with the critical value of J_2/J represents the critical point to which the nearest-neighbor model and all models with J_2 less than the critical value flow logarithmically slowly under renormalization. Therefore, we expect the behavior to be the same for the nearest-neighbor model up to logarithmic corrections.

D. Finite-size spectrum

The field theory model can now be used to calculate the finite-size spectrum of the spin chain at low energies. We first consider the case of periodic boundary conditions on a spin chain of even length l. This implies periodic boundary conditions on ϕ as in Eq. (2.28) and determines the mode expansion

$$\phi(x,t) = \phi_0 + \hat{\Pi}\frac{t}{l} + \hat{Q}\frac{x}{l} + \sum_{n=1}^{\infty}\frac{1}{\sqrt{4\pi n}}\left[e^{-(2\pi i/L)n(t-x)}a_n^L + e^{-(2\pi i/L)n(t+x)}a_n^R + \text{H.c.}\right]. \tag{2.42}$$

This implies that $\tilde{\phi}$ has the mode expansion

$$\tilde{\phi}(x,t) = \tilde{\phi}_0 + \hat{Q}\frac{t}{l} + \hat{\Pi}\frac{x}{l} + \sum_{n=1}^{\infty}\frac{1}{\sqrt{4\pi n}}\left[e^{-(2\pi i/L)n(t-x)}a_n^L - e^{-(2\pi i/L)n(t+x)}a_n^R + \text{H.c.}\right]. \tag{2.43}$$

The $a_n^{L,R}$'s are bosonic annihilation operators. $\hat{\Pi}$ and $\hat{Q}$ are canonically conjugate to the periodic variables ϕ_0 and $\tilde{\phi}_0$, respectively. Hence their eigenvalues are quantized

$$\hat{\Pi} = m/R, \quad \hat{Q} = 2\pi R\mathcal{S}^z, \tag{2.44}$$

with $\mathcal{S}^z$ and m integers. Note that $\tilde{\phi}$ is also periodic with radius $\tilde{R} = 1/2\pi R$. The resulting excitation spectrum is[11]

$$\begin{aligned} E = \int_0^l \mathcal{H}\,dx &= \frac{v}{2}\int_0^l \left[\Pi_\phi^2 + \left(\frac{\partial\phi}{\partial x}\right)^2\right] \\ &= \frac{v}{2}\left[\frac{\hat{\Pi}^2}{l} + \frac{\hat{Q}^2}{l} + \frac{2\pi}{l}\sum_{n=1}^{\infty} n\left(a_n^{L\dagger}a_n^L + a_n^{R\dagger}a_n^R\right)\right] \\ &= \frac{2\pi v}{l}\left[\frac{1}{2}\left(2\pi R^2(\mathcal{S}^z)^2 + \frac{m^2}{2\pi R^2}\right) + \sum_{n=1}^{\infty} n(m_n^L + m_n^R)\right] \end{aligned} \tag{2.45}$$

(We have reinserted the spin-wave velocity, v. $\mathcal{S}^z$ is the z component of the total spin.) The corresponding wave function is

$$\exp\left[i\left(\mathcal{S}^z 2\pi R\tilde{\phi}_0 + m\phi_0/R\right)\right]\prod_{n=1}^{\infty}(a_n^{L\dagger})^{m_n^L}(a_n^{R\dagger})^{m_n^R}|0\rangle. \tag{2.46}$$

We see from Eq. (2.23) that link parity takes $m \to -m$, $m_n^L \leftrightarrow m_n^R$, and multiplies the wave function by $(-1)^{\mathcal{S}^z+m}$. Here and in what follows, we always measure parity relative to that of the ground state. The ground-state parity itself for an even length chain is $(-1)^{l/2}$. This follows from the Perron-Froebenius theorem[12] for the nearest-neighbor model and we find numerically that it also holds for $J_2/J = 0.24$. At the point $J^z = 0$, $R = 1/\sqrt{4\pi}$, this spectrum is simply that of free fermions with antiperiodic (periodic) boundary conditions for even (odd) particle number.

If the number of sites l is odd, ϕ and $\tilde{\phi}$ obey *antiperiodic* boundary conditions. The mode expansions, spectrum, and wave functions are as in Eqs. (2.42), (2.45), and (2.46) except that now m and $\mathcal{S}^z$ are *half-odd integers*. Parity now simply takes $m \to -m$, $m_n^L \leftrightarrow m_n^R$. At the Heisenberg point the spin of left and right movers is separately conserved and the z components are given by

$$\mathcal{S}_{L,R}^z = (\mathcal{S}^z \pm m)/2. \tag{2.47}$$

The energy can then be written as

$$E = \frac{2\pi v}{l}\left[(\mathcal{S}_L^z)^2 + (\mathcal{S}_R^z)^2 + \sum_{n=1}^{\infty} n(m_n^L + m_n^R)\right]. \tag{2.48}$$

This spectrum has $\text{SU}(2)_L \times \text{SU}(2)_R$ symmetry for this value of R. Note, for instance, that for even l the lowest four excited states have quantum numbers $(s_L, s_R) = (\frac{1}{2}, \frac{1}{2})$, corresponding to a degenerate triplet and singlet under diagonal SU(2). [The spectrum consists of the highest weight representations of the $\text{SU}(2)_L \times \text{SU}(2)_R$ Kac-Moody algebras: $(s_L, s_R) = (0,0) + (\frac{1}{2}, \frac{1}{2})$ for l even and $(0, \frac{1}{2}) + (\frac{1}{2}, 0)$ for l odd. Parity simply interchanges all left and right quantum numbers and multiplies wave functions by (-1) in the $(\frac{1}{2}, \frac{1}{2})$ sector.]

We now turn to the case of free boundary conditions on the spins, corresponding to fixed boundary conditions on ϕ as in Eq. (2.31). The mode expansion is now

$$\phi(x,t) = 2\pi R\left(\frac{1}{2} + \mathcal{S}^z\frac{x}{l}\right) + \sum_{n=1}^{\infty}\frac{1}{\sqrt{\pi n}}\sin\left(\frac{\pi n x}{l}\right)\left[e^{-i\pi n t/l}a_n + \text{H.c.}\right] \tag{2.49}$$

with $\mathcal{S}^z$ an integer (half-odd integer) for l even (odd). The spectrum now takes the form[13]

$$E = \frac{\pi v}{l}\left[2\pi R^2(\mathcal{S}^z)^2 + \sum_{n=1}^{\infty} n m_n\right]. \tag{2.50}$$

Note that parity (i.e., $x \to l - x$) takes $a_m \to (-1)^m a_m$. It also multiplies wave functions by $(-1)^{\mathcal{S}^z}$ for l even. Thus

$$P = (-1)^{\sum_{p=0}^{\infty} m_{2p+1} + \mathcal{S}^z} = (-1)^{\sum_{p=1}^{\infty} p m_p + (\mathcal{S}^z)^2} \tag{2.51}$$

for l even. For l odd, $(\mathcal{S}^z)^2 - \frac{1}{4}$ is even, so we may write a similar formula:

$$P = (-1)^{\sum_{p=1}^{\infty} p m_p + (\mathcal{S}^z)^2 - 1/4}. \tag{2.52}$$

At the Heisenberg point this can simply be expressed in

TABLE I. Spectrum. (States accessible to our algorithm are underlined.)

$\frac{lE}{\pi v}$	Even periodic	Even open
0	$\underline{0^+}$	$\underline{0^+}$
1	$\underline{0^+}$, $\underline{1^-}$	$\underline{1^-}$
2	$\underline{1^+}$, 1^-	$\underline{0^+}$, $\underline{1^+}$
3	0^+, $\underline{0^-}$, 1^+, 1^-	$\underline{0^-}$, $2\times(1^-)$
4	$2\times(0^+)$, 0^-, 1^+, $2\times(1^-)$, $\underline{2^+}$	$2\times(0^+)$, $2\times(1^+)$, $\underline{2^+}$
5	$2\times(0^+)$, (0^-), $2\times(1^+)$, $3\times(1^-)$, 2^+, $\underline{2^-}$	$2\times(0^-)$, $4\times(1^-)$, $\underline{2^-}$
$\frac{lE}{\pi v}$	Odd periodic	Odd open
0	$\underline{\frac{1}{2}^+}$, $\underline{\frac{1}{2}^-}$	$\underline{\frac{1}{2}^+}$
1		$\underline{\frac{1}{2}^-}$
2	$2\times(\frac{1}{2}^+)$, $2\times(\frac{1}{2}^-)$, $2\times(\underline{\frac{3}{2}^+})$, $2\times(\underline{\frac{3}{2}^-})$	$\underline{\frac{1}{2}^+}$, $\underline{\frac{3}{2}^+}$
3		$2\times(\underline{\frac{1}{2}^-})$, $\underline{\frac{3}{2}^-}$
4	$4\times(\frac{1}{2}^+)$, $4\times(\frac{1}{2}^-)$, $3\times(\frac{3}{2}^+)$, $3\times(\frac{3}{2}^-)$	$3\times(\frac{1}{2}^+)$, $2\times(\frac{3}{2}^+)$
5		$4\times(\frac{1}{2}^-)$, $3\times(\frac{3}{2}^-)$

terms of the excitation energy

$$P=(-1)^{lE_{\rm ex}/v\pi}, \tag{2.53}$$

where the ground-state energy of $\pi v/4l$, for l odd, is subtracted from $E_{\rm ex}$; i.e., the energy levels are equally spaced and the parity simply alternates. Again we measure parity relative to the ground state. It follows from the Perron-Froebenius theorem that the ground-state site parity is $(-1)^{l/2}$ or $+1$ for an even- or odd-length open chain, respectively. [There is now a single SU(2) symmetry at the Heisenberg point corresponding to a single Kac-Moody algebra with the highest weight representation $s=0$ for l even and $s=\frac{1}{2}$ for l odd.]

The states of the first six energy levels are given in Table I for the four cases of even or odd l and periodic or open chain, indicating total spin and relative parity of the states.

III. QUANTUM IMPURITIES AND FINITE-SIZE SCALING

We will now use the theory of the previous section to predict the effect of various perturbations and impurities on the low-energy spectrum. The scaling dimension of the perturbing operators in the Hamiltonian is directly related to the finite-size scaling of the energy corrections to the low-energy spectrum.[7] If the dimension d of an operator is larger than one ($d>2$ if the operator is integrated over the whole chain rather than only appearing at one point), the perturbation is irrelevant because the corresponding coupling constant will renormalize proportional to l^{1-d}. This means that the energy corrections scale as l^{-d} and therefore go to zero faster than the asymptotic excitation energies, which scale as l^{-1}. Coupling constants of operators which have a scaling dimension which is less than one will again renormalize proportional to l^{1-d} as long as the coupling constant is small. Therefore, the corrections to the spectrum will increase relative to the asymptotic energy spacing, and the corresponding operator is relevant. Operators with dimension $d=1$ are marginal. Their coupling constant g will renormalize as $g(l)=g_0/(1-bg_0\ln l)\approx g_0+bg_0^2\ln l$ for small g_0. It now depends on the sign of the coupling constant if the perturbation is relevant or irrelevant. In any case, marginal operators give energy corrections that scale logarithmically slowly as $g(l)/l$.

It is now straightforward to test these predictions numerically. The isotropic Heisenberg model with a next-nearest-neighbor coupling of 0.24 times the nearest-neighbor coupling was used in most of the calculations. The "modified Lanczos" algorithm we used is briefly described in the Appendix. It determines the lowest energy in any sector of given quantum numbers. Since we consider local perturbations that destroy the translational symmetry of the periodic spin chain, momentum is not conserved. Thus, at best, we can find the lowest multiplet of given spin and parity. Furthermore, our algorithm does not keep track of the total spin but only the z component (see the Appendix). It is always possible to uniquely group the observed states into multiplets of definite spin. However, the lowest multiplet of given spin and parity may become unobservable when it lies higher in energy than another multiplet of higher spin and the same parity. (A way around this difficulty exists if one of the two multiplets has even integer spin and the other has odd integer spin. They are then distinguished by the spin-reversal symmetries of their $S^z=0$ members.)

A first test of the theory is to reproduce the finite-size spectrum of the periodic and open spin chains. Figures 5–8 show how well the numerically accessible states fit the predicted spectrum in Table I. In Table I we have underlined the multiplets which are accessible to our modified Lanczos technique. (We can find some additional states for the periodic chain by using translational invariance; however, once we include the impurity this possibility is lost.) A plot of the lowest-energy gap ver-

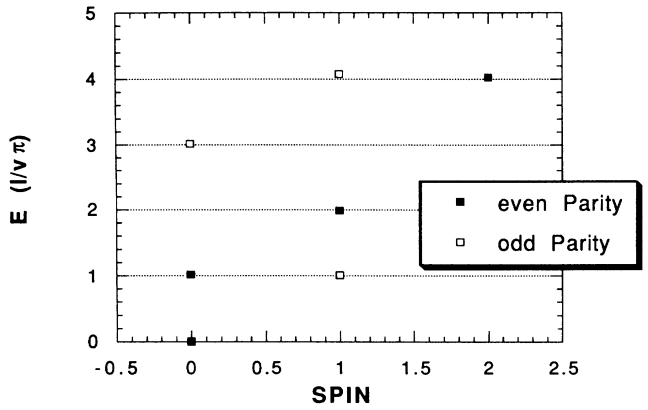

FIG. 5. Scaled numerical low-energy spectrum for a periodic, even-length (20) spin chain. The integer values $El/\pi v$ of the numerical accessible states agree with the theoretical predictions. The velocity $v\pi = 3.69$ was used (see Fig. 9).

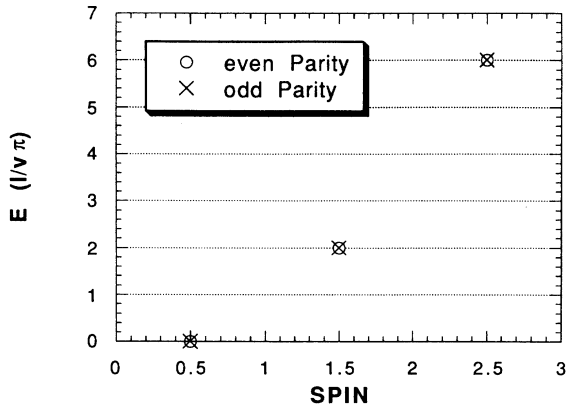

FIG. 6. Scaled numerical low-energy spectrum for a periodic, odd-length (19) spin chain ($v\pi = 3.69$).

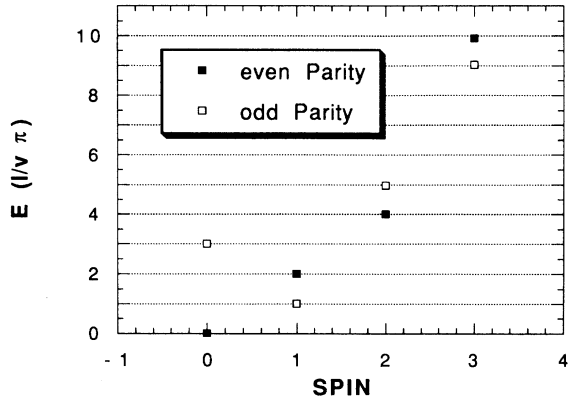

FIG. 7. Scaled numerical low-energy spectrum for an open, even-length (20) spin chain. The effect of the leading irrelevant operator T_L (a boundary energy operator), which gives l^{-2}-corrections as indicated in Fig. 10, is simply a length-dependent renormalization of the velocity. We therefore chose to scale with the velocity $v\pi = 3.65 - 4.6/l \approx 3.42$ in Figs. 7 and 8 only.

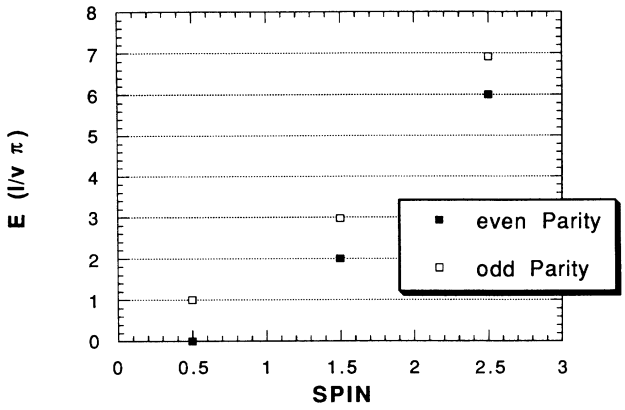

FIG. 8. Scaled numerical low-energy spectrum for an open, odd-length (19) spin chain ($v\pi = 3.42$).

sus length demonstrates the predicted $1/l$ dependence of energy gaps up to higher-order corrections from irrelevant operators (Figs. 9 and 10). Since we have tuned the marginal operator to zero, the lowest dimension bulk operator is $T_L T_R$ of dimension 4. Here $T_{L,R}$ is the left- (right) -moving part of the free Hamiltonian:

$$T_{L,R} \equiv \frac{1}{4}\left(\Pi_\phi \mp \frac{\partial \phi}{\partial x}\right)^2 . \tag{3.1}$$

This leads to $O(1/l^3)$ corrections to energy gaps for the periodic chain. For the open chain we also have a dimension 2 *boundary* operator, $\mathbf{J}_L \cdot \mathbf{J}_L \propto T_L$, leading to $O(1/l^2)$ corrections to energy gaps. This behavior is confirmed in Figs. 9 and 10.

Perhaps the simplest perturbation to consider is to introduce one weak coupling across the ends of the open chain (Fig. 1). The corresponding operator can be expressed as the product of two independent boundary spin operators. The continuum limit interaction becomes

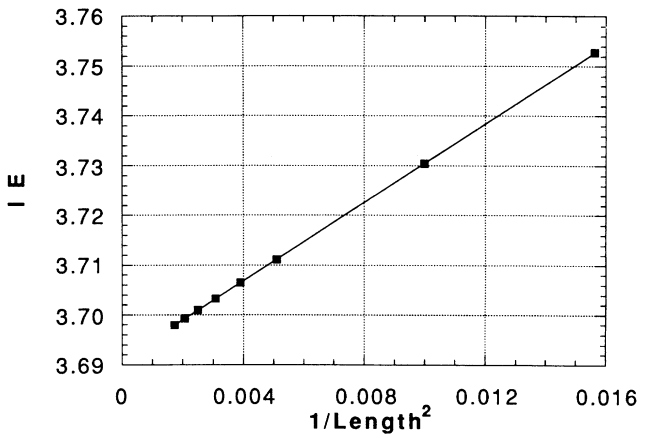

FIG. 9. Finite-size scaling towards an asymptotic spectrum for the periodic chain. The lowest excitation gap $0^+,1^-$ is fitted to $E = a/l + b/l^3$ for even lengths. Finite-size corrections to gaps therefore scale as l^{-3}. ($a = 3.69$, $b = 3.94$).

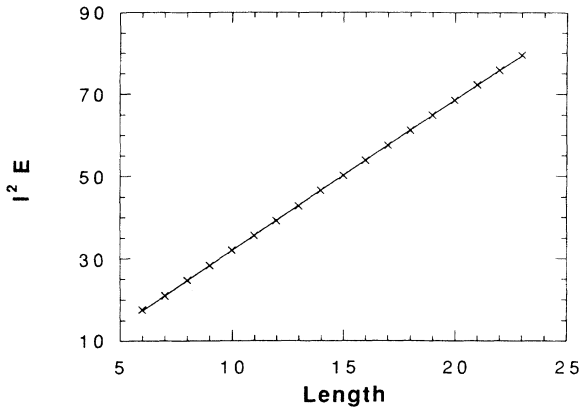

FIG. 10. Finite-size scaling towards an asymptotic spectrum for the open chain. The lowest excitation gap E is fitted to $E = a/l + b/l^2$ for both even and odd lengths. Finite-size corrections to gaps therefore scale as l^{-2}. ($a = 3.65$, $b = 4.6$).

$$\lambda\, \mathbf{S}_- \cdot \mathbf{S}_+ \propto \lambda\, \mathbf{J}_{L+} \cdot \mathbf{J}_{L-}. \tag{3.2}$$

Here $\pm$ represent the left and right sides of the weak link. (This notation should not be confused with the use of the superscripts $\pm$ to denote spin raising and lowering operators.) Assuming that we may regard the two sides of the link as completely independent in the limit $\lambda \to 0$ for a long chain, the dimension of this product of boundary operators is simply the sum of the dimensions, i.e., $d = 2$. We conclude that this perturbation is irrelevant, and therefore the open chain is a stable fixed point under this perturbation. We test this conclusion in Fig. 11. Here we consider a chain of odd length. For the open chain fixed point, the spectrum is given in Table I. The ground state has spin $s = \frac{1}{2}$, and the first excited state (at energy $v\pi/l$) also has $s = \frac{1}{2}$ with reversed parity. This lowest excitation energy, given in Fig. 11, shows very nicely that the corresponding energy corrections flow to zero with the predicted scaling of l^{-d}, ultimately giving back the open chain spectrum.

Alternatively, we can slightly alter the strength of one coupling somewhere in the periodic chain. We know from the previous section that the corresponding operator is $\mathrm{tr}g$, which has scaling dimension $d = \frac{1}{2}$ and is therefore relevant. Depending on the sign of the initial perturbation, the coupling will therefore increase or decrease more and more, until a stable fixed point is reached. In the case of decreasing coupling, this will be the open chain, while increasing coupling will produce a decoupled singlet together with an open chain with two sites removed. Figure 12 demonstrates again the predicted scaling l^{-d} of the energy corrections at a small coupling constant.

We chose chains of odd length, because, rather remarkably, Eqs. (2.48) and (2.49) predict that the excitation energies are identical for periodic and open even-length chains for all states accessible to our modified Lanczos technique; i.e., the lowest states of specified s and P. (See Table I.) Fortunately the situation is much better for odd l. The periodic chain has two degenerate doublet ground states of opposite parity, $\frac{1}{2}^{\pm}$, whereas the open chain has a single doublet ground state and a first excited state which is the reversed parity doublet with a gap $v\pi/l$. Thus we only need consider the two lowest-lying states. As a summary, Fig. 13 shows the dependence on the altered coupling of the first excitation energy for two different lengths, clearly indicating the two fixed points at coupling 0 and 1.

Since our bulk Hamiltonian contains first- and second-nearest-neighbor couplings we have chosen to maintain the ratio of second- to first-nearest-neighbor couplings of 0.24 while modifying the link. The three modified couplings are shown in Fig. 1. By doing this, we ensure that the open and periodic chains occur at zero and unit coupling, respectively. We also show the results of the Hamiltonian without the bulk next-nearest-neighbor

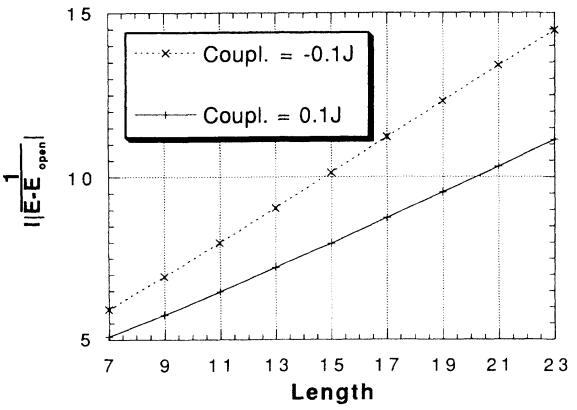

FIG. 11. Renormalization-group flow towards the open chain fixed point due to one weak link for an odd-length chain with $7 \le l \le 23$. The lowest excitation gap $\frac{1}{2}^+$, $\frac{1}{2}^-$ is fitted to $E - E_{\mathrm{open}} = 1/(al^2 + bl)$, exhibiting the predicted l^{-2} scaling corrections up to higher order.

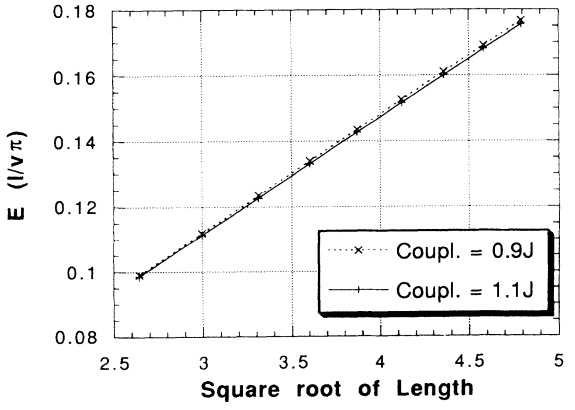

FIG. 12. Flow away from the periodic chain fixed point due to one altered link for an odd-length chain with $7 \le l \le 23$. The lowest excitation gap $\frac{1}{2}^+$,$\frac{1}{2}^-$ is fitted to $E = a/l^{1/2}$, which is the predicted scaling. (The parity of the two states interchanges at unit coupling.)

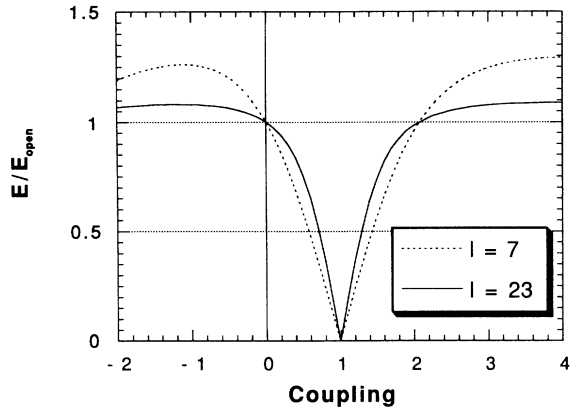

FIG. 13. The scaled excitation gap $\frac{1}{2}^+, \frac{1}{2}^-$ vs the coupling constant for one altered coupling for two different odd lengths. The parity of the two states reverses at unit coupling.

coupling present [i.e., $J_2 = 0$ in Eq. (2.41)] in comparison to our model $J_2 = 0.24J$ in Fig. 14. The qualitative behavior is the same for both models, but we see that the approach to the asymptotic behavior is much slower for the pure nearest-neighbor model because of logarithmic corrections (see Sec. II C).

A more interesting case involves altering two adjacent couplings by the same amount (Fig. 2). Starting from zero coupling, this can be incorporated by coupling an impurity spin to the two boundary operators at the ends of the open chain. The dimension at the Heisenberg point will simply be that of the boundary operators ($d = 1$), so we can expect marginal behavior. The perturbation becomes

$$H_{\rm int} = \lambda(\mathbf{S}_- + \mathbf{S}_+) \cdot \mathbf{S}_{\rm imp} \rightarrow \lambda(\mathbf{J}_{L+} + \mathbf{J}_{L-}) \cdot \mathbf{S}_{\rm imp}. \tag{3.3}$$

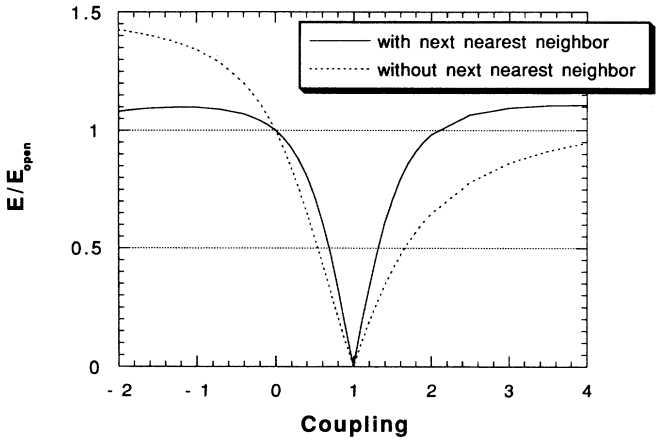

FIG. 14. Excitation gap $\frac{1}{2}^+, \frac{1}{2}^-$ vs the coupling constant for one altered coupling for the next-nearest-neighbor and pure nearest-neighbor bulk coupling models at a fixed length (19). The next-nearest-neighbor model scales faster to the fixed points because logarithmic corrections are not present.

Actually this case is equivalent to the Kondo problem which can also be written in the above form, in terms of current operators in an effective $(1 + 1)$-dimensional field theory. The resulting β function for the coupling constant λ is

$$\frac{d\lambda}{d(\ln l)} = \frac{\lambda^2}{v\pi}, \tag{3.4}$$

which tells us that the coupling will be marginally irrelevant for ferromagnetic sign ($\lambda < 0$) and marginally relevant for antiferromagnetic sign. The numerical results strongly support this picture. We plot the first excitation energy versus length in Figs. 15 and 16 for an odd total number of sites for ferromagnetic and antiferromagnetic couplings, respectively. In the ferromagnetic case, we approach the asymptotic spectrum consisting of an open even length chain together with a decoupled $s = \frac{1}{2}$ impurity. We can deduce this spectrum from Table I by simply taking a direct product of each multiplet in the "even open" section of the table with an $s = \frac{1}{2}$ variable. The first two energy levels have states: $\frac{1}{2}^+, \left[\frac{1}{2}^-, \frac{3}{2}^-\right]$. Here and in what follows, we put degenerate multiplets in square brackets. The corrections to this spectrum should only vanish as $1/l \ln l$. (There is also a $1/l^2$ correction, coming from the irrelevant operators $\mathbf{J}_+^2$, $\mathbf{J}_-^2$, and $\mathbf{J}_+ \cdot \mathbf{J}_-$. While this would be negligible for sufficiently long chains, it is fairly large for accessible lengths and therefore included in figures showing marginal flow.) The ferromagnetic coupling lowers the $\frac{3}{2}^-$ state relative to the $\frac{1}{2}^-$ state, which therefore becomes unobservable to our approach, as explained above. The $\frac{1}{2}^+, \frac{3}{2}^-$ gap is plotted in Fig. 15. It flows logarithmically slowly towards the open chain value, as expected. For antiferromagnetic coupling, the $\frac{1}{2}^-$ state is lower than $\frac{3}{2}^-$. The $\frac{1}{2}^+$, $\frac{1}{2}^-$ gap is plotted in Figure (16). For the fairly weak coupling used, it decreases from the open chain value in an approximately logarithmic fashion.

Starting from a periodic chain the corresponding operator for varying two adjacent sites by the

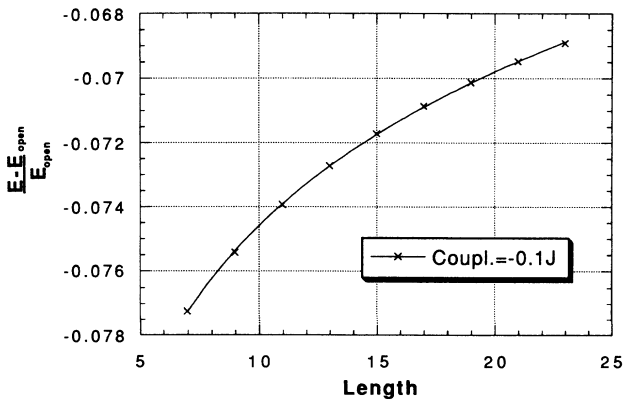

FIG. 15. Marginal flow towards the open chain fixed point due to two weak ferromagnetic links. Corrections to the $\frac{1}{2}^+, \frac{3}{2}^-$ gap are fitted to $E - E_{\rm open} = E_{\rm open}(a + b/l + c \ln l)$, demonstrating logarithmic scaling ($ac < 0$).

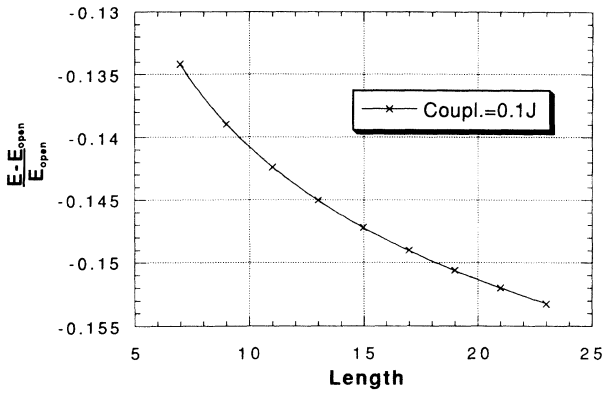

FIG. 16. Marginal flow away from the open chain fixed point due to two weak antiferromagnetic links. Corrections to the $\frac{1}{2}^+, \frac{1}{2}^-$ gap are fitted to $E - E_{\rm open} = E_{\rm open}(a + b/l + c \ln l)$, demonstrating logarithmic scaling ($ac > 0$).

same amount is the sum of two alternating operators $[{\rm tr}g(x) - {\rm tr}g(x+a)]$. This gives the derivative operator $\frac{d}{dx}{\rm tr}g$ of dimension $d = 1 + \frac{1}{2}$. This is lower in dimension than the uniform parts of the interaction ($d = 2$), but is still irrelevant. The predicted scaling of the $\frac{1}{2}^+, \frac{1}{2}^-$ gap with $l^{-3/2}$ is demonstrated in Fig. 17. At long lengths we recover the periodic chain spectrum with degenerate $\frac{1}{2}^\pm$ doublets. We see that when varying two adjacent couplings, the periodic chain is now a stable fixed point and the open chain with a decoupled spin is only stable for ferromagnetic perturbations. In the case of antiferromagnetic coupling to the impurity, the open chain will be unstable and ultimately flow to the stable periodic chain with the impurity site included. This results in a "healing" effect of the spin chain when we introduce any antiferromagnetic coupling on two equal adjacent links. These predictions are supported by the plot of excitation energy versus coupling for two different lengths in Fig. 18, clearly showing the two fixed points.

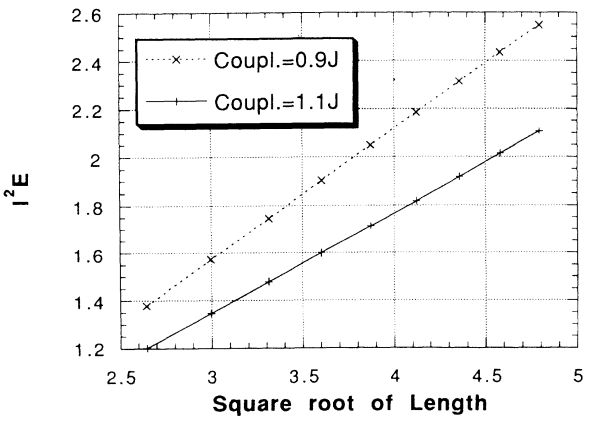

FIG. 17. Flow towards the periodic chain fixed point due to two altered antiferromagnetic links. The $\frac{1}{2}^+, \frac{1}{2}^-$ gap is fitted to $E = a/l^{3/2}$ which is the predicted scaling. The parity of the two states reverses at coupling one.

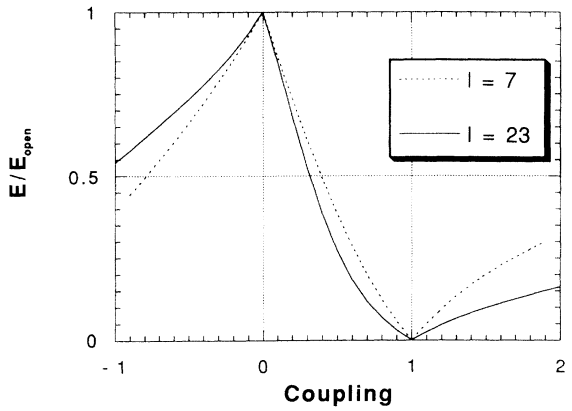

FIG. 18. Scaled excitation gap vs coupling for two altered equal adjacent couplings for two different odd lengths. The ground state always has $s = \frac{1}{2}$ while the excited state changes from $s = \frac{3}{2}$ for ferromagnetic coupling to $s = \frac{1}{2}$. The parity of the two states interchanges at coupling one.

At first sight one might be surprised that the alterations of one or two links in the chain have such fundamentally different effects. It is however exactly what we expect from the fundamentally different symmetries of the problems. A single modified link violates site parity and therefore permits the relevant operator tr$g$. However, having two equal adjacent weak links respects site parity, and therefore tr$g$ is not allowed. It does break link parity, thus allowing $\frac{d}{dx}{\rm tr}g$. We can readily understand the effect of various other, longer-range perturbations. Any perturbation which preserves site parity should be irrelevant, whereas any breaking of site parity is relevant (barring an accidental cancellation of the relevant operator). For instance, in our numerical work we modified the second-nearest-neighbor couplings to preserve the ratio $J_2/J = 0.24$ at the impurity site as shown in Figs. 1 and 2. Since this preserves link parity and site parity, respectively, in the two cases, it does not change our conclusions.

Both types of impurities that we have discussed above correspond to special cases of models studied in the context of defects in one-dimensional quantum wires.[4,5] In these papers spinless fermions were considered. This is equivalent to the xxz spin chain by the Jordan-Wigner transformation. The Heisenberg model corresponds to a particular value of the repulsive interaction. The flow of a single modified link to the open chain fixed point corresponds to the perfectly reflecting fixed point.[4] The "healing" discussed here corresponds to resonant tunneling.[5] In that work, it was necessary to adjust one parameter to achieve the resonance condition (even with exact site parity maintained). This parameter, a local chemical potential at the impurity site, corresponds to an external magnetic field term $h\, S_0^z$ at the impurity site. In the spin problem this is naturally set to zero by spin-rotation symmetry or time reversal. Thus resonance (healing) occurs without fine tuning in the spin chain.

We are now in the position to extend the analysis to

more general kinds of impurities by coupling spins of arbitrary magnitude in various ways to the spin chains. Maybe the most straightforward extension is to place an "internal" impurity of arbitrary spin inside the chain and then introduce two couplings of equal magnitude to the adjacent sites (Fig. 3). This is very much like the case we considered before, where the strength of two adjacent links was changed by the same amount. We expect the same marginal behavior at small coupling, but if the impurity does not have spin $\frac{1}{2}$, the chain cannot "heal" itself. We first consider the case of an $s = 1$ impurity, for example, a Ni^{2+} ion inserted into a Cu^{2+} chain. Ferromagnetic coupling is marginally irrelevant and the system will therefore slowly flow to the open chain with a decoupled $s = 1$ impurity as the length increases. For an even length chain with a spin-1 impurity, this fixed point gives us four lowest-lying states 1^+, $[2^-, 1^-, 0^-]$. We found the energies of the 1^+ and the 2^- states numerically, which demonstrate the predicted flow (Fig. 19) towards the stable open chain fixed point. Again it is important to consider the $1/l^2$ as well as the $1/l \ln l$ corrections. (The combined effect of the two terms actually produces an extremum in Fig. 19 at $l \approx 16$. Only for longer lengths does the logarithmic term dominate and the energy correction flow back to zero.)

Antiferromagnetic coupling is marginally relevant and increases slowly with length. We expect that the antiferromagnetic coupling will renormalize to infinity leading to a complete screening of the spin-1 impurity by the two neighboring spins and an open chain with two fewer spins. Starting from weak coupling we can trace the 1^+, 0^- states. The energy gap flows marginally away from the open chain fixed point value (Fig. 20). Eventually the two states cross, and at strong coupling the 0^- state will be the ground state and the energy gap to the 1^+ state again approaches the open chain fixed point value (Fig. 21). Note that the parity of the system is reversed because two sites are effectively removed from the chain. We expect the approach to the open chain fixed point to be governed by the same leading irrelevant operator as before $\mathbf{J}_{L-} \cdot \mathbf{J}_{L+}$ of dimension 2.

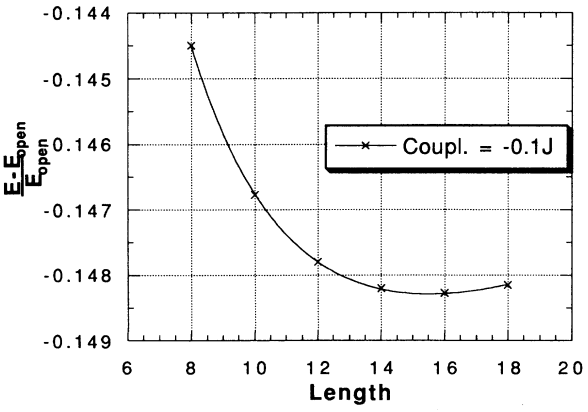

FIG. 19. Renormalization flow for the weak ferromagnetic coupling to an internal $s = 1$ impurity. Corrections to the 1^+,2^- gap are fitted to $E - E_{\text{open}} = E_{\text{open}}(a + b/l + c \ln l)$, demonstrating logarithmic scaling ($ac < 0$).

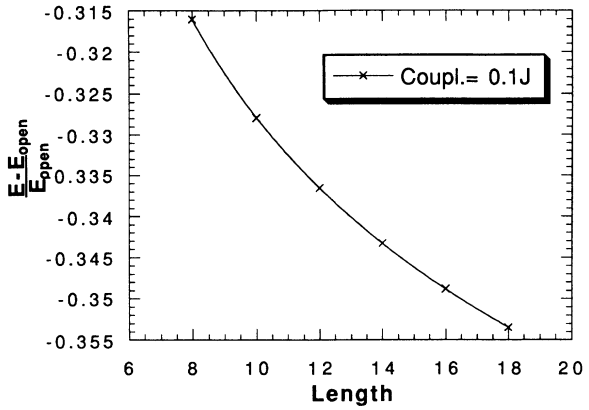

FIG. 20. Renormalization flow for the weak antiferromagnetic coupling to an internal $s = 1$ impurity. Corrections to the 1^+,0^- gap are fitted to $E - E_{\text{open}} = E_{\text{open}}(a + b/l + c \ln l)$, demonstrating logarithmic scaling ($ac > 0$).

Now consider the case of $s = \frac{3}{2}$. Since ferromagnetic coupling is marginally irrelevant, we expect to obtain the open chain fixed point with a decoupled spin-$\frac{3}{2}$ impurity as the stable fixed point. The antiferromagnetic case is more subtle. If we assume that the couplings to the impurity renormalize to infinity, we obtain an effective impurity of size $\frac{1}{2}$. This effective impurity then couples to the next pair of spins in the chain. Whether this effective defect heals or decouples depends on the sign of the effective coupling. Note that if we assume that the direct impurity couplings are infinite, then the effective spin is antiparallel to the screening spins (see Fig. 22). Consequently the antiferromagnetic couplings to the screening spins correspond to a *ferromagnetic* coupling to the effective impurity. Thus we are led naturally to the hypothesis that the effective coupling will always be ferromagnetic and hence we flow to the open chain fixed point with a decoupled $s = \frac{1}{2}$. This argument extends immediately to higher s. The stable fixed point is always the open chain

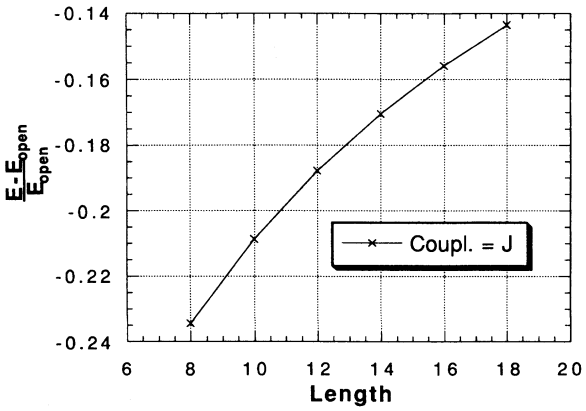

FIG. 21. Renormalization flow for strong antiferromagnetic coupling to an internal $s = 1$ impurity. Corrections to the 0^-,1^+ gap flow to the open chain value $E - E_{\text{open}} = 0$.

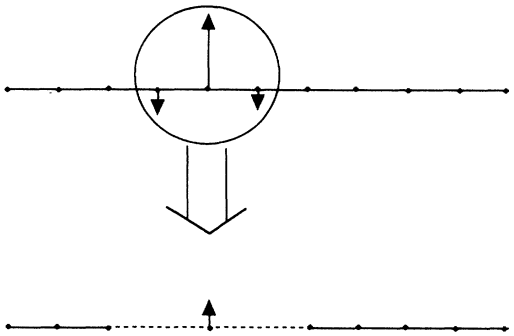

FIG. 22. Sign of coupling to the partially screened effective spin is reversed.

with a decoupled impurity of size s in the ferromagnetic case and $s-1$ in the antiferromagnetic one.

We will now imagine an "external" impurity of spin s, placed outside a periodic chain and coupled to just one site in the chain (Fig. 4). In this case, we are dealing with a bulk spin operator coupled to a (dimensionless) impurity spin. The continuum limit interaction Hamiltonian is now

$$H_{\rm int} = i\lambda\,{\rm tr}\,[g\,\sigma]\cdot\mathbf{S}_{\rm imp}. \tag{3.5}$$

This interaction has dimension $\frac{1}{2}$. It is *relevant for either sign of the coupling*, unlike the case of the internal

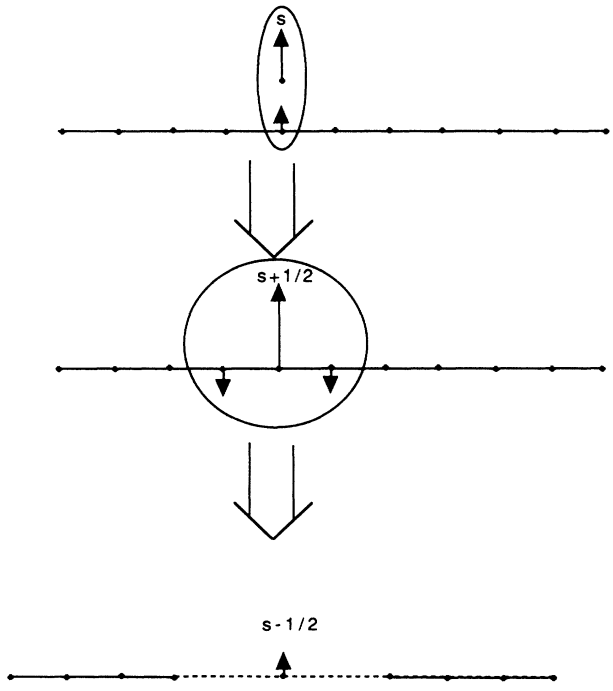

FIG. 23. External spin of size s with ferromagnetic coupling produces a spin of size $s+\frac{1}{2}$. This is coupled antiferromagnetically to its neighbors and hence gets screened to size $s-\frac{1}{2}$. The resulting coupling is then ferromagnetic and therefore flows to zero.

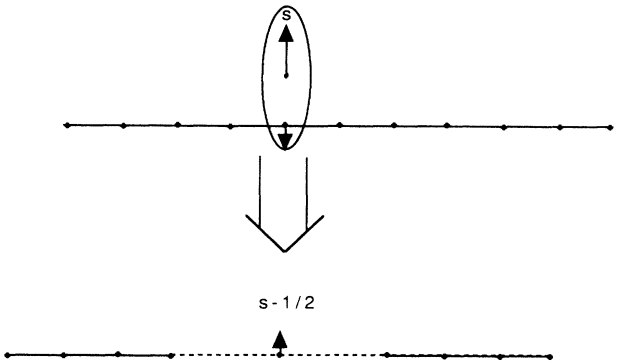

FIG. 24. External spin of size s is partially screened to size $s-\frac{1}{2}$ for antiferromagnetic coupling. The effective coupling of this partially screened spin to its neighbors is ferromagnetic and therefore flows to zero.

impurity. For ferromagnetic coupling we expect that the impurity will couple strongly to spin $\frac{1}{2}$ in the chain and play the role of an antiferromagnetically coupled "internal" impurity of spin $s+\frac{1}{2}$, which then will get screened to size $s-\frac{1}{2}$ and eventually decouple as described above. The screening process is depicted in Fig. 23. For antiferromagnetic coupling the impurity will get screened directly by the spin in the chain, thereby also making the coupling to the rest of the chain ferromagnetic by the same argument employed above for an internal impurity (see Fig. 22). Hence the screened impurity decouples from the chain as shown in Fig. 24. Ultimately we will flow to an open chain with a decoupled impurity of spin $s-\frac{1}{2}$ for either sign of the coupling, with the fixed points only differing in the effective number of spin sites, which is lowered by three for ferromagnetic coupling and by one for antiferromagnetic coupling from the original chain length. Note that this kind of impurity changes odd- to even-length chains and vice versa.

For an external spin-$\frac{1}{2}$ impurity coupled to an odd-

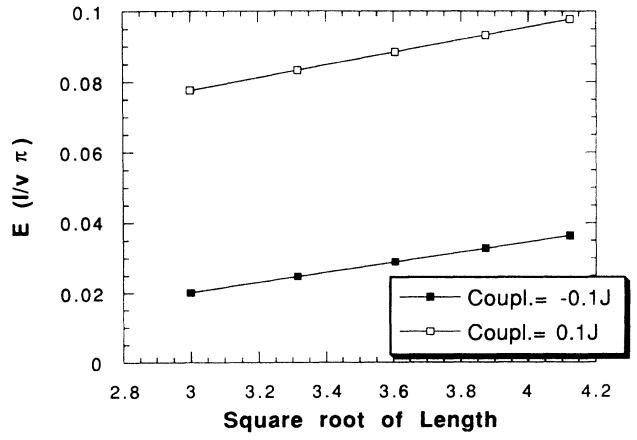

FIG. 25. Flow away from the periodic chain fixed point due to weak coupling to an external $s=\frac{1}{2}$ impurity. The $0^+,1^-$ gap is fitted to $E=a/l^{1/2}+b/l$ exhibiting the predicted $l^{-1/2}$ scaling corrections up to higher order. For ferromagnetic coupling the parity of the two states is reversed.

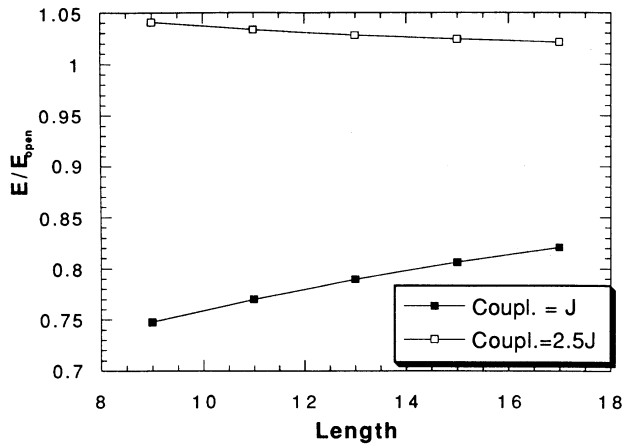

FIG. 26. Flow to the open chain of a periodic chain with strong antiferromagnetic coupling to an external $s = \frac{1}{2}$ impurity. The $0^+,1^-$ gap approaches the open chain fixed point value $E = E_{\text{open}}$.

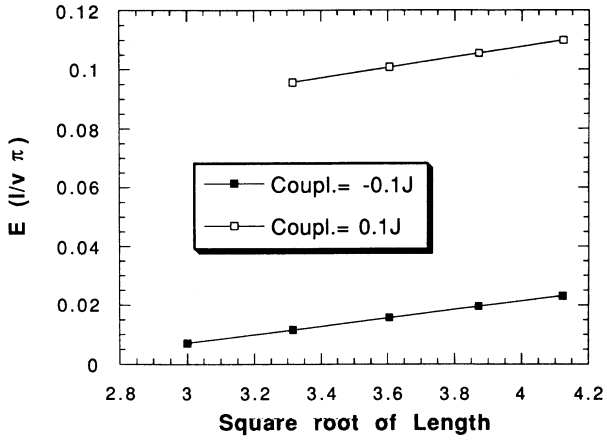

FIG. 27. Flow away from the periodic chain fixed point due to weak coupling to an external $s = 1$ impurity. The $\frac{1}{2}^+,\frac{3}{2}^-$ gap is fitted to $E = a/l^{1/2} + b/l$ exhibiting the predicted $l^{-1/2}$ scaling corrections up to higher order. For antiferromagnetic coupling the parity of the two states is reversed.

length chain, we expect the effective internal impurity to be of spin 0, so that the two lowest-lying states are simply those of the even-length open chain $(0^+, 1^-)$. Numerically we find exactly these two lowest-lying states, moving away from the periodic chain behavior $E = 0$ with the predicted relevant scaling and slowly approaching the open chain fixed point spectrum (Figs. 25 and 26).

For an external impurity of spin 1 coupled to an odd-length chain, the fixed point is an $s = \frac{1}{2}$ impurity with an even-length open chain, so that the lowest-lying states are $\frac{1}{2}^+, \left[\frac{3}{2}^-, \frac{1}{2}^-\right]$. Again we find the two lowest-lying states $\frac{1}{2}^+$ and $\frac{3}{2}^-$ numerically for either sign of the coupling, with their energy difference moving away from the zero-coupling periodic chain value $E = 0$ with the predicted scaling (Fig. 27). There is a parity reversal of the states when going from ferromagnetic (three sites removed) to antiferromagnetic coupling (one site removed), which is not indicated explicitly in the graphs.

IV. THERMODYNAMICS

In this section we discuss the thermodynamics of a single impurity in a quantum spin chain. We first consider the scaling limit in which $T \to 0$ and $l \to \infty$. In practice this means $T \ll v$ and $T \ll T_K$, where T_K is the "Kondo temperature," i.e., the energy scale at which renormalization-group flow to the stable fixed point occurs. It also means $l \gg 1$ and $l \gg v/T_K$. In this limit, the partition function only depends on the dimensionless ratio v/lT. In the presence of a magnetic field h, it also depends on the other dimensionless ratio h/T. Corrections to these results are expressed in a perturbative series in the irrelevant operators and are suppressed by powers of T/T_K.

We begin by considering the scaling limit. The partition function for an open xxz chain with anisotropy corresponding to a radius R is

$$Z^{e,o}_{\text{open}}(lT/v; R) = \sum_{S^z} \exp[-(\pi v/lT)(2\pi R^2)(S^z)^2] \prod_{m=1}^{\infty} [1 - \exp(-\pi v m/lT)]^{-1}. \tag{4.1}$$

The sum over S^z runs over integers or half-integers for an even or odd length, corresponding to Z^e and Z^o, respectively. Note that Z is a product of the contributions of the soliton degree of freedom S^z with a rigid rotator spectrum, and of the harmonic oscillator degrees of freedom a_m. In the low-temperature limit, $lT/v \to 0$, the partition function is dominated by the lowest-energy state; i.e., a singlet for even length or a doublet for odd length. In the opposite limit, $lT/v \to \infty$, we find the asymptotic behavior

$$Z \to \frac{1}{\sqrt{4\pi}R} e^{\pi lT/6v + O(v/lT)} \tag{4.2}$$

for an even *or* odd length. In this limit the free energy consists of a bulk term, scaling with l plus an l-independent impurity contribution. The bulk free energy gives a linear specific heat:

$$c_{\text{bulk}}(T) = \pi lT/3v. \tag{4.3}$$

The impurity free energy simply gives a temperature-independent entropy $S = \ln g$, where the "ground-state degeneracy" g is given by

$$g(R) = \frac{1}{\sqrt{4\pi}R}. \tag{4.4}$$

Note that there is no impurity contribution to the specific heat in this limit. This only arises when we include

irrelevant operator contributions. Taking into account the doubling of degrees of freedom for the periodic chain, we find that in this case the partition function is given by

$$Z^{e,o}_{\text{periodic}}\left(\frac{lT}{v},R\right)$$

$$= Z^{e,o}_{\text{open}}\left(\frac{lT}{2v},\frac{R}{\sqrt{2}}\right) Z^{e,o}_{\text{open}}\left(\frac{lT}{2v},\frac{1}{2\sqrt{2}\pi R}\right). \tag{4.5}$$

In the limit $lT/v \to \infty$, we find

$$Z^{e,o}_{\text{periodic}}(lT/v,R) \to e^{\pi lT/6v+O(v/lT)}. \tag{4.6}$$

Note that the bulk part of the free energy (that scales with l) is the same as for the open chain. However, there is no "impurity free energy" in this case; the ground-state degeneracy is $g(R)=1$ for all R.

The ground-state degeneracy $g(R)$ is in general non-integer for the open chain. It is only integer at the free fermion point $g(1/\sqrt{4\pi})=1$. These systems provide interesting examples of the "g theorem" which was conjectured but only partially proven perturbatively in Ref. 2. This theorem states that g always decreases under renormalization from a less stable to a more stable boundary fixed point. It is in many ways analogous to Zamolodchikov's[15] "c theorem" which states that the conformal anomaly parameter c, proportional to the specific-heat slope, also decreases under renormalization between bulk fixed points. The flows between the various fixed points that we have discussed all obey this theorem. Let us begin by considering the Heisenberg model for which $g=1/\sqrt{2}<1$ for the open chain. We saw in the previous section that modifying one weak link is a relevant perturbation which drives the system from the periodic to open chain. In this process g decreases from 1 to $1/\sqrt{2}$, respecting the g theorem. For two weak links the flow is from the open to periodic chains. However, in this case, the unstable open chain fixed point also contains a decoupled impurity spin. This contributes an extra factor of 2 to g, $g=2/\sqrt{2}>1$. Thus again g decreases under renormalization.

It is interesting to consider the general xxz chain from this perspective. For the case of one weak link, the lowest-dimensional operators at the periodic and open chain fixed points have dimensions $1/4\pi R^2$ and $4\pi R^2$, respectively. Thus the stability of the fixed points reverses when R passes through $1/\sqrt{4\pi}$, the xx point, corresponding to a free fermion. (This was observed in Ref. 4. It corresponds to a transition between perfect reflection and perfect transmission when the fermion interactions change sign from repulsive to attractive.) We note that the ground-state degeneracy for the open chain passes through 1 at precisely the same value of R, so that the flow is always in the direction of decreasing g. (Despite the fact that the change in g is small near the free Fermion point, this *does not* provide an example to which the perturbative proof of the g theorem[2] applies. That proof assumed a barely relevant coupling constant λ with β function $\frac{d\lambda}{d\ln l}=y\lambda-b\lambda^2$, where b is of order 1 and $y \ll 1$. In this case b vanished in the limit $y \to 0$, as we approach the free Fermion fixed point. Since this happens, the boundary operator is a modified hopping term in the free Fermion Hamiltonian and there is no nonlinear β function in a free theory.)

Next we consider the magnetization in the scaling limit, i.e., ignoring irrelevant operators. We specialize to the Heisenberg case for an open chain. Now only the rigid rotor degrees of freedom contribute, giving

$$M = T\frac{\partial}{\partial h}\ln\left(\sum_{S^z}\exp[-(\pi v/lT)(S^z)^2+(h/T)S^z]\right). \tag{4.7}$$

(Again the sum is over integer or half-integer S^z for even or odd chains, respectively.) In the low-temperature limit, the susceptibility vanishes exponentially for an even-length chain: $\chi \to (2/T)e^{-\pi v/lT}$, but exhibits Curie law behavior for an odd-length chain due to the $s=\frac{1}{2}$ ground state: $\chi \to 1/4T$. In the infinite length limit, the magnetization exhibits only a bulk term: $M \to lh/2\pi v$; there is no impurity magnetization, ignoring irrelevant operators.

Now we consider the effect of irrelevant operators. We work in the infinite length limit and consider the specific heat and susceptibility. These calculations exactly parallel the fairly well-known ones that have been done for the Kondo effect.[14] We simply perform lowest-order perturbative calculations in the leading irrelevant operator. Because these operators are irrelevant, all higher-order corrections are suppressed by additional powers of T compared to the leading-order calculation. The power of T, with which the specific heat and susceptibility scale, is determined by the dimension of the leading irrelevant operator. The behavior is somewhat different depending on whether the periodic or open chain is the stable fixed point.

Let us first consider the open chain fixed point. There are now three leading irrelevant operators, all of dimension 2: $\mathbf{J}_+^2$, $\mathbf{J}_-^2$, and $\mathbf{J}_+\cdot\mathbf{J}_-$. We expect the corresponding coupling constants to be of order $1/T_K$, where T_K is the energy scale at which the crossover to the stable fixed point occurs. If we slightly perturb the periodic chain with one modified link by δJ, for example, we expect $T_K \propto (\delta J)^2/v$ since the relevant operator has dimension $\frac{1}{2}$. The impurity specific heat is proportional to T/T_K, since it arises from first-order perturbation theory in the leading irrelevant operator. Note that this is dimensionless, as is the bulk term $\pi lT/3v$. The factor of l/v is replaced by $1/T_K$ in the impurity term. By the same reasoning, we predict an impurity susceptibility proportional to $1/T_K$, T-independent at $T \to 0$. Again this has the same dimension as the bulk term, $l/2\pi v$, with l/v replaced by $1/T_K$.

Next we consider the periodic chain fixed point, which is stable in the case of two modified links. In this case the leading irrelevant operator $(d/dx)\text{tr}g$ has dimension $\frac{3}{2}$. Thus the corresponding coupling constant is $1/T_K^{1/2}$. If we begin with an almost decoupled spin with coupling δJ to its two neighbors, then the Kondo temperature is ex-

ponentially small: $T_K \propto e^{-\text{const}\cdot v/\delta J}$. The leading irrelevant operator can also be written as $(\mathbf{J}_{L,-1}+\mathbf{J}_{R,-1})\cdot \mathrm{tr} g\boldsymbol{\sigma}$. It is convenient to regard the right-moving spin degrees of freedom as a second channel of left movers, for purposes of doing perturbation theory in the boundary operator. We then have two left-moving $k = 1$ WZW fields. This is equivalent to a single $k = 2$ WZW field together with an Ising sector, a correspondence which was used in a discussion of the two-impurity Kondo effect.[16] The operator $\mathrm{tr} g\boldsymbol{\sigma} \rightarrow g_1^{\alpha}\boldsymbol{\sigma}_{\alpha}^{\beta}g_{2\beta} \rightarrow \boldsymbol{\phi}$, where $\boldsymbol{\phi}$ is the spin-1 primary field in the $k = 2$ theory of dimension $\frac{1}{2}$. The leading irrelevant operator becomes $\mathbf{J}_{-1}\cdot\boldsymbol{\phi}$. This is precisely the same leading irrelevant operator as occurs in the two-channel Kondo effect. Thus we can take over the results of Ref. 1 directly. $\mathbf{J}_{-1}\cdot\boldsymbol{\phi}$ is a primary field with respect to the single Virasoro algebra in the purely left-moving theory. Therefore, its finite-temperature expectation value vanishes. Consequently, the leading contribution to the specific heat arises from *second-order* perturbation theory. The second-order perturbation theory result gives an impurity specific heat

$$c_{\text{imp}} \propto (T/T_K)\ln(T/T_K). \tag{4.8}$$

Similarly, the impurity susceptibility has a logarithm

$$\chi_{\text{imp}} \propto \ln(T/T_K). \tag{4.9}$$

For the periodic chain fixed point, the Wilson ratio R_W is universal because there is only one leading irrelevant operator. We find

$$R_W \equiv \frac{\chi_{\text{imp}}/c_{\text{imp}}}{\chi_{\text{bulk}}/c_{\text{bulk}}} = \frac{8}{3}. \tag{4.10}$$

V. CONCLUSIONS

We have studied the effect of various types of impurities in $s = \frac{1}{2}$ Heisenberg antiferromagnets. In nearly all cases we found that the stable fixed point is the open chain, sometimes with a leftover decoupled partially screened impurity. The only exception is the case of two weak links where the periodic chain is the stable fixed point, corresponding to a healing of the defect.

There are analogies to both the single-channel and the two-channel Kondo effects. The most striking difference is that the two fixed points that occur in the single-channel Kondo problem (0 or $\pi/2$ phase shift) are equivalent, whereas the open and periodic spin-chain fixed points are quite different from each other. The open chain fixed point is very similar to the single-channel Kondo fixed point. The Kondo interaction (corresponding to coupling open chains to an isolated impurity) is marginal. In the absence of a decoupled spin, the leading irrelevant operator is of dimension 2. On the other hand, the periodic chain fixed point is more like the non-Fermi-liquid fixed point that occurs in the two-channel $s = \frac{1}{2}$ Kondo effect, despite the fact that it corresponds to a trivial boundary condition (i.e., no boundary condition) on the spin chain. The reason for this is that both left- and right-moving channels come into play. The healing process that we have described is analogous to overscreening in the Kondo effect. The two neighboring spins overscreen the $s = \frac{1}{2}$ impurity, leading to an effective impurity of the same size, which is then screened by the next pair of spins, etc. Beginning from the limit of two very weak links, the fixed point occurs at a value of the couplings which is neither zero nor ∞, as in the two-channel Kondo case. The leading irrelevant operator is actually equivalent to the one occurring in the two-channel Kondo problem.

Although the discussion so far has focussed on the case of an $s = \frac{1}{2}$ chain, much of it should apply to general half-integer spin. The continuum limit of the Heisenberg model is believed to be the same for all half-integer spins.[17] Thus all the above conclusions from the continuum limit about the relevance or irrelevance of various perturbations and about finite-size scaling carry over directly. The generalization of the healing phenomena to higher spin merits some discussion. It is clear that equally modifying two-neighboring bonds will always be irrelevant and lead to healing. What is less clear is what will occur if a *smaller* spin is inserted into the chain, for example, an $s = \frac{1}{2}$ impurity in an $s = \frac{3}{2}$ chain. This is again an "overscreened" situation. If the antiferromagnetic couplings flow to infinity, the effective spin becomes $\frac{5}{2}$. The effective coupling to the next pair of spins remains antiferromagnetic. If this coupling flows to infinity, then the effective spin becomes $\frac{1}{2}$ again, etc. Thus it is natural to hypothesize that the system will always flow to some critical point which *does not* correspond to the open chain, whenever an impurity of size s_{impurity} is inserted into a half-odd-integer-spin chain such that $2s_{\text{chain}} > s_{\text{impurity}}$. The stable critical point might correspond to the periodic chain (as it does for $s_{\text{chain}} = s_{\text{impurity}} = \frac{1}{2}$) or may possibly be a nontrivial fixed point.

Experimental observation of the effects discussed here will probably not be easy. Two crucial effects which we have not discussed are interimpurity interactions and interchain couplings. The former are rather analogous to Ruderman-Kittel-Kasuya-Yosida (RKKY) interactions in the Kondo effect. They are relevant for arbitrarily low impurity concentration in the one-dimensional case, based on replica methods.[18] In order to study quenched random disorder, an approximate renormalization-group transformation has been developed[19,20] in which most strongly antiferromagnetically coupled pairs of spins are eliminated, leaving behind only weak couplings between the spins on either side of the pairs. This tends to produce a progressively more dilute system of spins with weaker couplings. It leads to a susceptibility which diverges at $T \rightarrow 0$, but less rapidly than $1/T$. It is unclear to us whether this approximation takes into account the effects which we have discussed here for a single impurity. It seems less appropriate in the dilute impurity limit, where most spins form long uniform chains and more strongly coupled pairs essentially do not exist. This question may deserve further investigation.

Another possibility for observing the effects discussed here is in muon spin-resonance experiments. In this case,

the muon itself may act as the impurity, and it is perfectly feasible to study a single impurity.

ACKNOWLEDGMENTS

We would like to thank Matthew Fisher and Andreas Ludwig for interesting discussions and the Supercomputing Division of the Environment Canada Meteorological Centre for use of their NEC SX3/44 supercomputer. This research was supported in part by NSERC of Canada.

APPENDIX: THE ALGORITHM

The algorithm we used starts from a normalized initial trial vector Ψ_1 and successively minimizes the energy expectation value in each iteration step by forming the linear combination $\tilde{\Psi}_2 = b\Psi_1 + H\Psi_1$. The explicit formulas are

$$b = \frac{1}{2\Delta_2}(\Delta_3 - \sqrt{\Delta_3^2 + 4\Delta_2\Delta_4}), \tag{A1}$$

$$\Psi_2 = \frac{b\Psi_1 + H\Psi_1}{(b^2 + 2b\langle H\rangle + \langle H^2\rangle)^{1/2}}, \tag{A2}$$

where

$$\Delta_2 = \langle H^2\rangle - \langle H\rangle^2, \tag{A3}$$
$$\Delta_3 = \langle H\rangle\langle H^2\rangle - \langle H^3\rangle, \tag{A4}$$
$$\Delta_4 = \langle H^2\rangle^2 - \langle H\rangle\langle H^3\rangle. \tag{A5}$$

We used the notation $\langle H^n\rangle = \langle\Psi_1|H^n|\Psi_1\rangle$. The energy is given by

$$\langle\Psi_2|H|\Psi_2\rangle = \langle H\rangle - \frac{\sqrt{\Delta_3^2 + 4\Delta_2\Delta_4}}{b^2 + 2b\langle H\rangle + \langle H^2\rangle}. \tag{A6}$$

The algorithm terminates when we are close to the ground state so that the energy cannot be lowered much further. Clearly all symmetries of Ψ_1 are preserved in each step, so the algorithm can be used to find ground states in different sectors of H.

We decided to work in the orthonormal S_z basis because the next-nearest-neighbor coupling requires excessive computations in the valence-bond basis,[21] which keeps track of the total spin. The basis states can be represented by integer bitstrings, and the Hamiltonian was implemented as a procedure that manipulates and then stores the bitstrings and their coefficients as they are created. For numerical convenience we used the exchange Hamiltonian, which differs by a factor of 2 and a constant from the Heisenberg Hamiltonian. The various tricks to optimize the algorithm include a hashing technique,[22] extrapolation to the exact ground state, and reusing previously created information on how to update basis states. The resulting ground state can be used as an initial starting state for a similar Hamiltonian with only slightly modified parameters. The extrapolation is based on the fact that the actual ground-state energy is approached exponentially and simply uses the last three iteration values to find an improved result. (This gives reliably at least two more digits accuracy.)

Taking into account the limited available symmetries of our problem, we can handle only about 22 sites on a SUN workstation (about 8 sites less than what can be done for a periodic chain in the valence-bond basis). Some calculations were done on a NEC SX3/44 supercomputer because supercomputers generally allow for about four more sites. Working in the valence-bond basis with $s = 0$ and using translational and parity invariance, we can find the exact ground state to 8-digit accuracy of a periodic chain of 24 sites in only 15-sec CPU time on a NEC SX3/44 supercomputer. This needs to be compared to 20-min CPU time on a SPARCstation2 when working in the S_z basis for the same problem.

[1] I. Affleck, Nucl. Phys. **B336**, 517 (1990); I. Affleck and A.W.W. Ludwig, *ibid.* **B352**, 849 (1991); **360**, 641 (1991); A.W.W.Ludwig and I. Affleck, Phys. Rev. Lett. **67**, 3160 (1991).

[2] I. Affleck and A.W.W. Ludwig, Phys. Rev. Lett. **67**, 161 (1991).

[3] T. Kennedy, J. Phys. Condens. Matter **2**, 5737 (1990); I. Hagiwara, K. Katsumata, I. Affleck, B.I. Halperin, and J.P. Renard, Phys. Rev. Lett. **65**, 3181 (1990); S.H. Glarum, S. Geschwind, K.M. Lee, M.L. Kaplan, and J. Michel, *ibid.* **67**, 1614 (1991).

[4] C.L. Kane and M.P.A. Fisher, Phys. Rev. Lett. **68**, 1220 (1992).

[5] C.L. Kane and M.P.A. Fisher (unpublished).

[6] J.L. Cardy, Nucl. Phys. **B324**, 581 (1989).

[7] J.L. Cardy, Nucl. Phys. **B270**, 186 (1986).

[8] For a review and a list of original references for the Jordan-Wigner transformation and bosonization see, for example, I. Affleck, *Fields Strings and Critical Phenomena*, edited by E. Brézin and J. Zinn-Justin (North-Holland, Amsterdam, 1990), p. 563.

[9] I. Affleck, D. Gepner, H. Schulz, and T. Ziman, J. Phys. A **22**, 511 (1989).

[10] F.D.M. Haldane, Phys. Rev. Lett. **60**, 635 (1988).

[11] F.C. Alcarez, M.N. Barber, and M.T. Batchelor, Phys. Rev. Lett. **58**, 771 (1987); I. Affleck and J.B. Marston, J. Phys. C **21**, 2511 (1988).

[12] The proof is a simple generalization of the proof of ground-state uniqueness in E. Lieb, T. Schultz, and D. Mattis, Ann. Phys. (N.Y.) **16**, 407 (1961).

[13] F.C. Alcarez, M. Baake, U. Grimm, and V. Rittenberg, J. Phys. A **21**, L117 (1988).

[14] P. Nozières, *Proceedings of the 14th International Conference on Low Temperature Physics*, edited by M. Krusius and M. Vuorio (North-Holland, Amsterdam, 1974), Vol. 5, p. 339.

[15] A.B. Zamolodchikov, JETP Lett. **43**, 730 (1986).

[16] I. Affleck and A.W.W. Ludwig, Phys. Rev. Lett. **68**, 1046

(1992).
[17]F.D.M. Haldane, Phys. Lett. **93A**, 464 (1983); I. Affleck and F.D.M. Haldane, Phys. Rev. B **36**, 5291 (1987).
[18]C.A. Doty and D.S. Fisher, Phys. Rev. B **45**, 2167 (1992).
[19]C. Dasgupta and S.-K. Ma, Phys. Rev. B **22**, 1305 (1980).
[20]J.E. Hirsch, Phys. Rev. B **22**, 5355 (1980); J.E. Hirsch and J.V. José, *ibid.* **22**, 5339 (1980).
[21]For a review of the valence-bond basis see K. Chang, I. Affleck, G.W. Hayden, and Z.G. Soos, J. Phys. **1**, 153 (1989).
[22]E.R. Gagliano, E.D. Moreo, A. Moreo, and F.C. Alcaraz, Phys. Rev. B **34**, 1677 (1986).